POLARIMETRIC CHARACTERISTICS OF FULLY POLARIZATION SAR IMAGE OBSERVED BY GROUND-BASED SAR SYSTEM

Moon-Kyung Kang[1*], Kwang-Eun Kim[2], Hoonyol Lee[3], Seong-Jun Cho[4] and Jae-Hee Lee[5]

[1] Korea Institute of Geoscience and Mineral Resources, Daejeon, Republic of Korea, kangmk@kigam.re.kr
[2] Korea Institute of Geoscience and Mineral Resources, Daejeon, Republic of Korea, kimke@kigam.re.kr
[3] Kangwon National University, Suncheon, Republic of Korea, hoonyol@knu.ac.kr
[4] Korea Institute of Geoscience and Mineral Resources, Daejeon, Republic of Korea, mac@kigam.re.kr
[5] Korea Institute of Geoscience and Mineral Resources, Daejeon, Republic of Korea, zack@kigam.re.kr

ABSTRACT: Ground-Based SAR system that obtains a high resolution 2D image on the ground is a new type of SAR system such as air-borne and space-borne SAR. The measured fully polarimetric SAR images with HH, HV, VH, and VV were focused using the Deramp-FFT (DF) algorithm in terms of their image formation principles. SAR polarimetry technique is concerned with control of the polarimetric properties of radar waves and the extraction of target properties from the behaviour of scattered waves from a target. In this study, we processed the polarimetric SAR data obtained by the GB-SAR system to investigate the polarimetric characteristics of terrain targets such as trees, grass and several permanent scatterers located in the test site. The polarimetric classification images using H/A/Alpha polarimetric decomposition and Wishart algorithms were extracted and discussed for deriving a scattering property according to different target types.

KEY WORDS: GB-SAR, fully polarimetric SAR, SAR polarimetry, target decomposition

1. INTRODUCTION

Ground-Based SAR (GB-SAR) systems were interested in monitoring tools for agriculture, terrain mapping, man-made structures and concentrated on these studies related to ground surface deformation detection and displacement measurement of structures like dams, bridges, and so on. And most of these applications and studies of GB-SAR system were based on SAR interferometric techniques. For analysis of more detailed physical and biophysical features of various surface targets on the earth's surface, we need to understand scattering characteristics received from single or distributed targets. Many researchers have been interested in classification, decomposition, and modelling of polarimetric SAR data in recent literature. The objective behind efforts is better understanding about the scattering mechanism that give rise to the polarimetric characteristics seen in SAR image data.

Nowadays polarimetric target decomposition theorems in SAR polarimetry are recognized an important SAR polarimetric technique for an interpretation based on physical constraints. In general, target decomposition theorem can be divided four categories: 1) those based on the dichotomy of the Kennaugh matrix (Huynen, Holm and Barnes, Yang), 2) those based on a 'model-based' decomposition of the covariance matrix or the coherency matrix (Freemann and Durden, Yamaguchi), 3) those using an eigenvector or eigenvalues analysis of the covariance matrix or coherency matrix (Cloude, Holm, van Zyl, Cloude and Pottier), and 4) those employing coherent decomposition of the scattering matrix (Krogager, Cameron, Touzi). Those using an eigenvector or eigenvalues analysis of the covariance matrix or the coherency matrix are the most generally used method to analyzing of polarimetric information about a single or distributed target. Cloude and Pottier proposed the entropy (H) based classification method for extracting average parameters from polarimetric SAR data using an eigenvector and eigenvalues of the 3×3 Hermitian averaged coherency matrix (Cloude and Pottier, 1997). The principal polarimetric scattering parameters of H/A/Alpha polarimetric decomposition theorem are entropy (H), alpha (α), and anisotropy (A). The value of alpha parameter can be easily related with the physics behind the scattering process. The entropy H determines the degree of randomness of the scattering process, which can be also interpreted as the degree of statistical disorder. In the limit case, when H=1, the polarization information becomes zero and the target scattering is truly a random noise process and when H=0, the scattering process corresponds to a pure target. The polarimetric anisotropy that measures the relative importance of the second and the third eigenvalues of the decomposition is a parameter complementary to the entropy H.

In this paper, we present our recent efforts to analyzing the dominant scattering properties about different surface targets such as trees, grasses, a human-made structure, and several permanent scatterers located in the study area using H/A/Alpha polarimetric decomposition algorithms. This work was focused on application study of the developed GB-SAR system based on SAR polarimetry techniques as a preliminary study.

2. METHODOLOGY

The employed GB-SAR instrumentation consists of a Vector Network Analyzer (VNA) working at C-band (5.3

㎓), a linear horizontal rail where the antennas move for scanning the synthetic aperture, and a notebook computer controlling the VNA, the motion of the antennas, the data recording. This GB-SAR system that could be operated on fully polarimetric SAR imaging system was developed by Korea Institute of Geoscience and Mineral Resources (KIGAM) and Kangwon National University over the past several years. The polarimetric SAR data composed HH, HV, VH, and VV was measured on 160 times during 3 days between 3rd and 5th November, 2008. The obtained SAR data was presented '#_no' in the order. The used GB-SAR system characteristics are shown in Table 1.

The test site (shown in Figure 1) that purposed for the GB-SAR system operation and performance test was located inside Korea Institute of Geoscience and Mineral Resources (KIGAM) field. Five permanent scatterers were located on grasses. And other natural target such as trees and grasses and several terrestrial magnetic measurement boxes were included in this area shown in Figure 1.

Table 1. GB-SAR system measurement characteristics.

Center Frequency	5.3 ㎓
Range Bandwidth	600 ㎒
IF BW	1 ㎑
Number of Point	1601
Power	VNA 0 dBm, Amp 33 dBm
Azimuth Step	5 cm
Azimuth Length	5 m
Polarization	HH, HV, VH, VV

Figure 1. A front view photo of test site.

We used the 'gbsar' processor developed by Kangwon National University for the SAR focusing. Already the characteristics, advantage, and limitations of the used DF algorithm and the RD algorithm were compared to find an efficient SAR focusing method (Lee et al., 2007a; Lee et al., 2007b). In this work, the SAR data focused by DF algorithm were processed for analyzing of polarimetric characteristics related to natural or man-made different terrain targets such as a permanent target, trees, grasses, and man-made structures. After SAR focusing processing, the polarimetric SAR images were processed using the open software package, called PolSARpro that is developed to provide by the end an educational software which could offer a tool for self-education in the field of polarimetric SAR data analysis, and to be accessible to a wide range of users, from novices to experts in the field of polarimetry and interferometric polarimetric SAR data processing (http://envisat.esa.int/polsarpro/).

We focused on analysis of polarimetric segmentation and classification using H/A/Alpha target decomposition algorithms. And we consider that other polarimetric target decomposition algorithms such as Freeman and Durden 3 component (Freeman and Durden, 1998) and Yamaguchi 3, 4 components decompositions (Yamaguchi et al., 2005) based on a model-based decomposition of the covariance matrix or the coherency matrix and Stokes parameters, correlation coefficients, phase difference, reflectivity ratio, differential reflectivity, and so on will be applied in the future work.

3. RESULTS

Figure 2 shows an RGB color coded image correspond |S11|, |S12|, and |S22| components of #_1. As shown in Figure 2, we can indicated that black and green colored areas for trees group in the middle region, strong signal features at 5 permanent scatterers location in the upper and right part, and several blue colored spotty areas in the right part of the image. These spotty areas were presumed that soaked with water. Figure 3 displays three HH, HV, and VV amplitude images in dB. 5 permanent scatterers and trees features were appeared more dominantly in HH and VV images as shown in Figure 3(a) and (c). And the soaked area as black spotty pattern was appeared at HH polarization in the upper right part of Figure 3(a) clearly. In the case of HV polarization image, the whole image show more uniformly feature than HH and VV images.

Figure 4 shows the atmosphere temperature variation graph (a) and the phase variation graph (b) of each HH, HV, VH, and VV polarizations measured at a permanent scatterer location (ps_1) during entire measurement times between #_1 and #_160. The totally graph distribution of Figure 4(a) and (b) tend to be similar. From these graphs results we selected on 3 maxima (#_7, #_80, and #_155) and 2 minima (#_56 and #_130) positions which may be reflected environmental effect varied depending on temporal and other atmospheric factors.

Figure 5, 6, 7, and 8 show classification images in the case of #_1, #_7, and #_56 after applying polarimetic segmentation using H/A/Alpha algorithms with Wishart classifier method. We can indicate that the images applied H/A/Alpha segmentation method can be provide more detailed classification information than H/Alpha results. Also we can consider that atmospheric factors need to be analyzed for interpretation and analysis of polarimetric SAR data. The classification results of #_1, #_7, and #_56 that showed a little different classification pattern, in particular, in the trees and grass area.

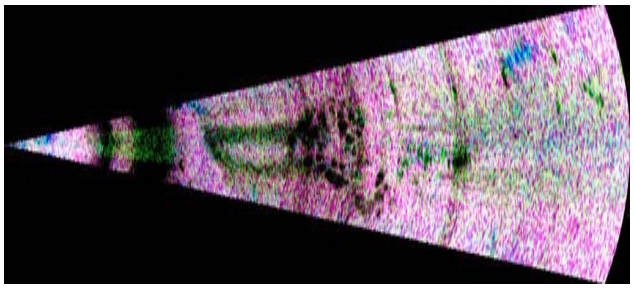

Figure 2. An example of RGB (as |S22|, |S12|, and |S11|) color composite polarimetric image after geocoding.

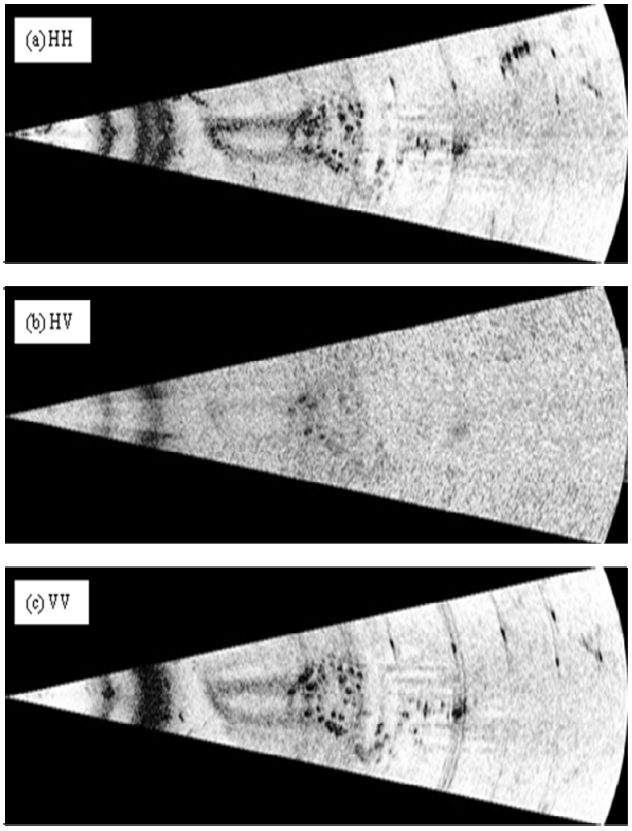

Figure 3. Amplitude images (in dB) for HH, HV, and VV polarization (#_1).

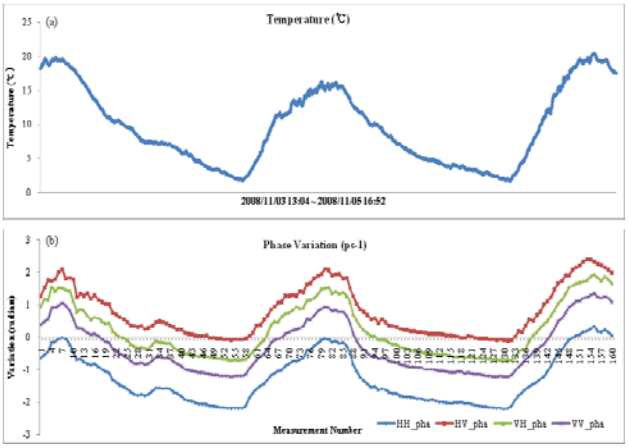

Figure 4. Atmosphere temperature variation (a) and phase variation (b) at a permanent scatterer (ps_1) during 160 measurement times.

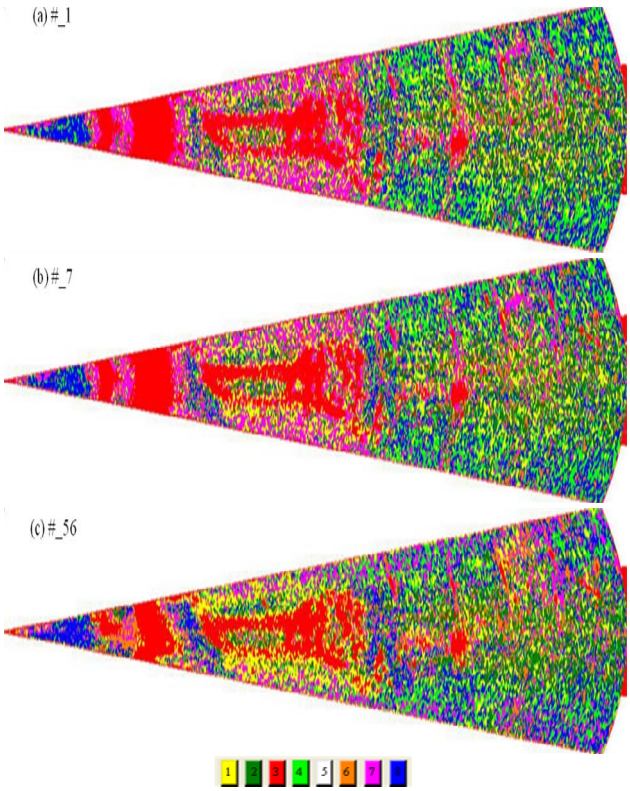

Figure 5. Classification results after applying H/Alpha and the Wishart classifier applied for 10 iterations by 3 windows: (a) #_1, (b) #_7, and (c) #_56.

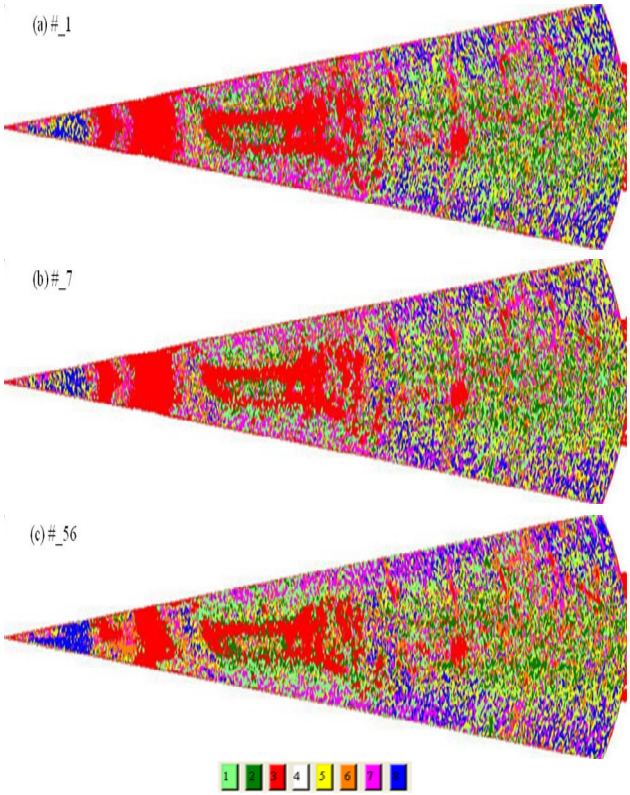

Figure 6. Classification results after applying H/Alpha1 and the Wishart classifier applied for 10 iterations by 3 windows: (a) #_1, (b) #_7, and (c) #_56.

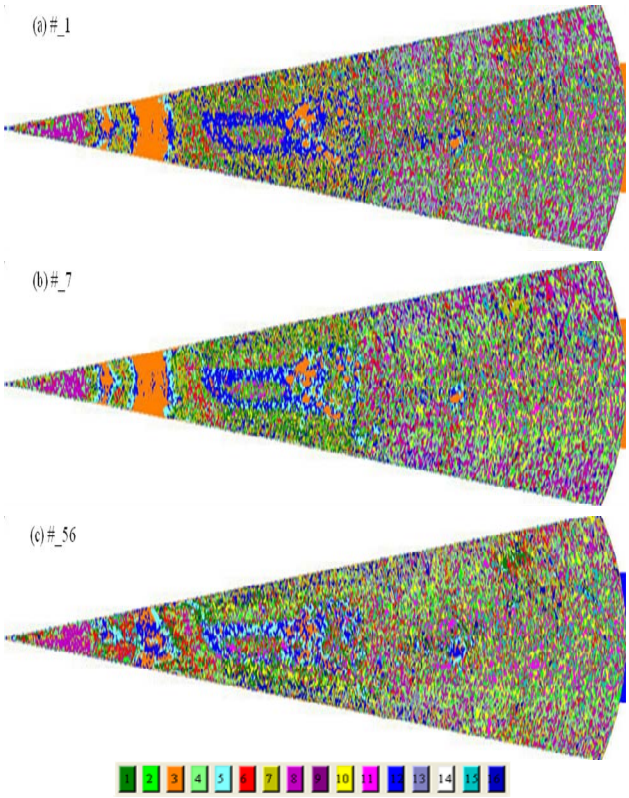

Figure 7. Classification results after applying H/A/Alpha and the Wishart classifier applied for 10 iterations by 3 windows: (a) #_1, (b) #_7, and (c) #_56.

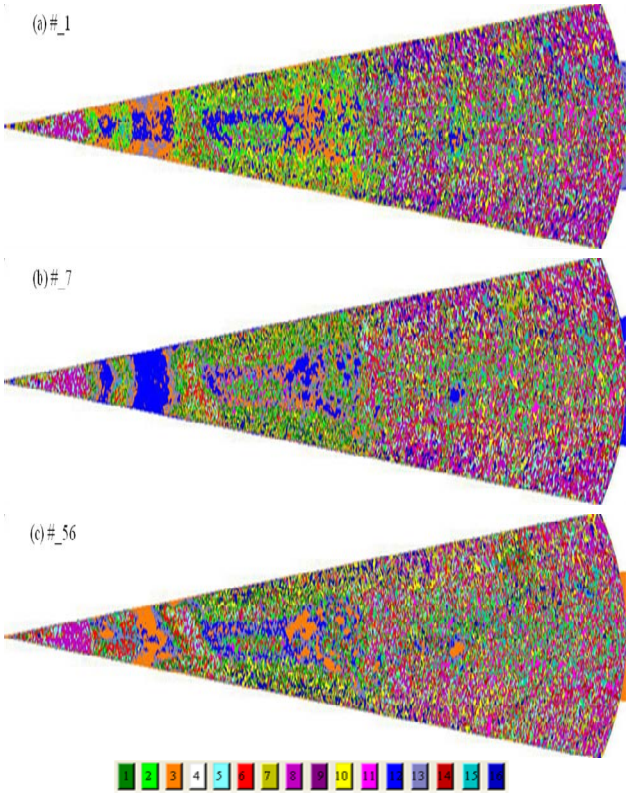

Figure 8. Classification results after applying H/A/Alpha1 and the Wishart classifier applied for 10 iterations by 3 windows: (a) #_1, (b) #_7, and (c) #_56.

4. CONCLUSIONS

The objective of this study has been to assess a geophysical application of fully polarimetric SAR data measured by the GB-SAR system in order to extracting relevant information about surface scattering properties. From the classification results, we can consider that the dominant scattering property of different surface targets such as natural or man-made targets varies depending on target's material types and their environmental conditions like roughness, moisture, and so on. We thought that an environmental factor and temporal analysis will be need investigated for extracting more detailed polarimetric information of various targets in the future research.

5. REFERENCES

Cloude, S. R. And Pottier, E, 1997. An Entropy Based Classification Scheme for Land Applications of Polarimetric SAR, *IEEE Transactions on Geosciences and Remote Sensing, 35(1)*, pp. 68-78.

Freeman, A. And Durden, S. L., 1998. A Three-Component Scattering Model for Polarimetric SAR Data, *IEEE Transactions on Geosciences and Remote Sensing, 35(1)*, pp. 963-973.

Lee, J.-S. and Pottier, E., 2009. Polarimetric Radar Imaging From Basics to Applications, CRC Press.

Lee, H., Cho, S.-J., Sung, N.-H., and Kim, J.-H., 2007a. Development of a GB-SAR (I): System Configuration and Interferometry, *Korean Journal of Remote Sensing*, 23(4), pp. 237-245.

Lee, H., Cho, S.-J., Sung, N.-H., and Kim, J.-H., 2007b. Development of a GB-SAR (II): Focusing Algorithms, *Korean Journal of Remote Sensing*, 23(4), pp. 247-256.

Yamaguchi, Y., Moriyama, T., Ishido, M., and Yamada, H., 2005. *IEEE Transactions on Geosciences and Remote Sensing, 43(8)*, pp. 1699-1706.

6. ACKNOWLEDGEMENTS

This research was supported by a grant (07KLSGC03) from Cutting-edge Urban Development - Korean Land Spatialization Research Project funded by Ministry of Land, transport and Maritime Affairs of Korean government.